

# Spin-photon interaction in a nanowire quantum dot with asymmetrical confining potential

Rui Li (李睿) <sup>1, \*</sup>

<sup>1</sup>*Key Laboratory for Microstructural Material Physics of Hebei Province,  
School of Science, Yanshan University, Qinhuangdao 066004, China*

(Dated: February 12, 2024)

The electron (hole) spin-photon interaction is studied in an asymmetrical InSb (Ge) nanowire quantum dot. The spin-orbit coupling in the quantum dot mediates not only a transverse spin-photon interaction, but also a longitudinal spin-photon interaction due to the asymmetry of the confining potential. Both the transverse and the longitudinal spin-photon interactions have non-monotonic dependence on the spin-orbit coupling. For realistic spin-orbit coupling in the quantum dot, the longitudinal spin-photon interaction is much (at least one order) smaller than the transverse spin-photon interaction. The order of the transverse spin-photon interaction is about 1 nm in terms of length  $|z_{eg}|$ , or 0.1 MHz in terms of frequency  $eE_0|z_{eg}|/h$  for a moderate cavity electric field strength  $E_0 = 0.4$  V/m.

## I. INTRODUCTION

The spin degree of freedom of electron or hole confined in semiconductor quantum dot can be utilized to design a qubit, the building block of a quantum computer [1–4]. The single spin manipulation is achievable by using the electric-dipole spin resonance technique in quantum dot with spin-orbit coupling [5–11], and the two-spin manipulation is achievable by using the exchange interaction in a double quantum dot [12, 13]. Spin qubit also inevitably interacts with the surrounding electric [14, 15], magnetic [16, 17], and phonon environments [18, 19], such that there exist both spin relaxation and spin dephasing. The theory of lattice phonons induced spin relaxation in semiconductor quantum dot has been well established [18, 19]. Also, several potential mechanisms of the charge noise induced spin dephasing were proposed recently [20–22].

The quantum theory of a two-level system interacting with cavity photons has been well built in quantum optics [23]. The basic models include the Jaynes-Cummings model [24] and the Rabi model [25]. There is an increasing interest in studying the spin-photon interaction in semiconductor quantum dot [26–36], due to its potential application in achieving the long distance two spin interaction [37, 38]. The spin-orbit coupling in semiconductor quantum dot provides a natural coupling mechanism for the spin and photons. A one-dimensional (1D) cavity, i.e., a transmission line resonator [39, 40], is mainly used in current experiments [41–45]. It is more convenient to achieve the strong system-photon interaction in a 1D cavity than in a traditional 3D cavity [39].

The quantum states of a nanowire quantum dot can be solved exactly even in the presence of strong spin-orbit coupling [21, 22, 46], such that it is possible to unveil novel spin-orbit coupling effect in this simple sys-

tem. Previous studies obtained only a transverse spin-photon interaction in a nanowire quantum dot with symmetrical confining potential [8, 26]. Here, we study the effects of the asymmetry of the confining potential [47] on the spin-photon interaction. We obtain exactly both the eigen-energies and the eigenstates of an asymmetrical quantum dot. In the Hilbert subspace spanned by the lowest two eigenstates, we obtain a general spin-photon interaction Hamiltonian, in which in addition to the usual transverse spin-photon interaction [26, 28], there is also a longitudinal spin-photon interaction. Both the transverse and the longitudinal spin-photon interactions have non-monotonic dependence on the spin-orbit coupling. The emergence of the longitudinal interaction is due to the combined effects of the spin-orbit coupling and the asymmetrical confining potential [21, 22]. For typical spin-orbit coupling and typical parameters of the quantum dot, the longitudinal interaction is at least one-order smaller than the transverse interaction. Although the longitudinal spin-electric interaction demonstrated here is too weak to affect the quantum information transfer between the spin and photons, it does provide a possible mechanism for the spin dephasing induced by the charge noise [21, 22].

## II. SPIN-PHOTON INTERACTION HAMILTONIAN

The system under investigation is schematically shown in Fig. 1. The undoped InSb (Ge) nanowire can be populated with electrons (holes) from the ohmic contacts via applying positive (negative) voltage to the backgate, i.e., the  $p^{++}$  doped Si substrate [48]. An electron (hole) can be trapped in the InSb [48, 49] (Ge) [50, 51] nanowire quantum dot via applying proper voltages to the three bottom gates 1-3 [see Fig. 1(a)]. The quantum dot setup is also placed in a 1D transmission line resonator [39–45], where the nanowire is placed to be perpendicular to the center conductor and pointing to the ground plane of

\* [rui.li@ysu.edu.cn](mailto:rui.li@ysu.edu.cn)

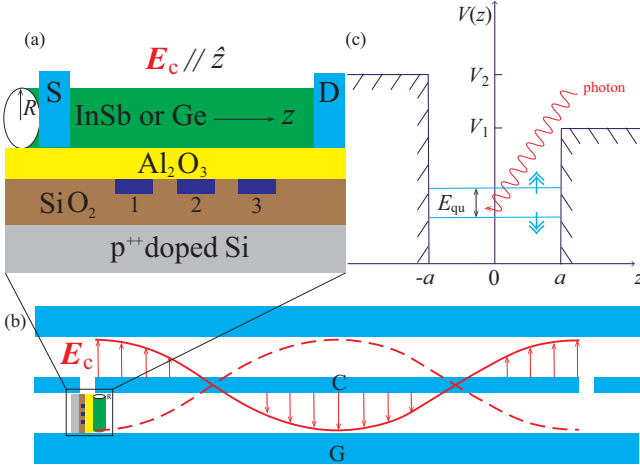


FIG. 1. (a) A possible InSb or Ge nanowire quantum dot setup. The  $p^{++}$  doped Si substrate is covered with  $\text{SiO}_2$ , three bottom gates 1-3 for creating the quantum dot confining potential are buried under  $\text{Al}_2\text{O}_3$ , on which an InSb or Ge nanowire is deposited. The contacts between the nanowire and source/drain are ohmic. (b) The quantum dot setup is also placed in a transmission line resonator, and the cavity electric field  $\mathbf{E}_c$  is along the nanowire axis, i.e., the  $z$  direction. (c) An asymmetrical square well with heights  $V_{1,2}$  and width  $a$  is used to model the quantum dot confining potential. The spin basis states are just the lowest two eigenstates of the quantum dot.

the transmission line resonator [see Fig. 1(b)]. The total Hamiltonian of this coupled quantum-dot-cavity system reads

$$H = \hbar^2 k_z^2 / (2m) + \alpha \sigma^x k_z + \delta \sigma^z + V(z) + e z E_0 (b + b^\dagger) + \hbar \omega_c b^\dagger b, \quad (1)$$

where  $m$  is the effective electron/hole mass,  $\alpha$  is the spin-orbit coupling strength,  $\delta$  is half of the Zeeman energy,  $E_0$  is the strength of the cavity electric field  $\mathbf{E}_c$ ,  $\omega_c$  is the cavity frequency,  $b$  ( $b^\dagger$ ) is the bosonic annihilation (creation) operator for the cavity mode, and  $V(z)$  is the quantum dot confining potential modeled by an asymmetrical square-well [see Fig. 1(c)]

$$V(z) = \begin{cases} V_2, & z < -a, \\ 0, & |z| < a, \\ V_1, & a < z, \end{cases} \quad (2)$$

with  $V_{1,2}$  and  $a$  characterizing the well heights and the well width, respectively. Note that in our following calculations, unless otherwise stated, we have set the square well parameters as  $a = 40$  nm,  $V_1 = 5$  meV, and  $V_2 = 8$  meV.

Our strategy of obtaining the effective spin-photon interaction Hamiltonian is as follows. First, we obtain exactly the basis states of the spin qubit, i.e., the lowest two eigenstates  $|\Psi_{e,g}\rangle$  of the quantum dot Hamiltonian  $H_{\text{qu}} = \hbar^2 k_z^2 / (2m) + \alpha \sigma^x k_z + \delta \sigma^z + V(z)$ , i.e., the first line of Eq. (1). Note that as long as  $V(z)$  is a square

well potential, the quantum dot Hamiltonian  $H_{\text{qu}}$  is exactly solvable [21, 22, 46, 52], although  $H_{\text{qu}}$  contains non-trivial spin-orbit coupling physics. Second, in the Hilbert subspace spanned by the qubit basis states  $|\Psi_{e,g}\rangle$ , we calculate the matrix form of the electric-dipole operator  $ez$  shown in Eq. (1). Finally, we are able to obtain an effective spin-photon interaction Hamiltonian  $H_{\text{ef}}$ , that can be written explicitly as

$$H_{\text{ef}} = \frac{E_{\text{qu}}}{2} \tilde{\sigma}^z + e E_0 (b + b^\dagger) \left[ \left( \frac{z_{ee} + z_{gg}}{2} + \frac{z_{ee} - z_{gg}}{2} \tilde{\sigma}^z \right) + |z_{eg}| (\tilde{\sigma}^x \cos \varphi_{eg} + \tilde{\sigma}^y \sin \varphi_{eg}) \right] + \hbar \omega_c b^\dagger b, \quad (3)$$

where  $E_{\text{qu}}$  is the level splitting of the spin qubit,  $\tilde{\sigma}^{x,y,z}$  are the Pauli matrices defined in the qubit Hilbert subspace,  $z_{ee} = \langle \Psi_e | z | \Psi_e \rangle$ ,  $z_{gg} = \langle \Psi_g | z | \Psi_g \rangle$ , and  $z_{eg} = |z_{eg}| \exp(i\varphi_{eg}) = \langle \Psi_e | z | \Psi_g \rangle$ . Although the matrix element  $z_{eg}$  has both amplitude  $|z_{eg}|$  and phase  $\varphi_{eg}$ , the strength of the transverse interaction only depends on the amplitude  $|z_{eg}|$ .

The effective interaction Hamiltonian (3), in which there are both longitudinal and transverse spin-photon interactions, can be regarded as a general spin-boson model in quantum optics. The strength of the spin-photon interaction is certainly proportional to the cavity electric field strength  $E_0$ . The realistic  $E_0$  is related to the frequency of cavity and some other parameters of the transmission line [39], and its typical value is about  $E_0 = 0.4$  V/m [39]. However, this value may be improvable by future experimental advances, such that in the following we use  $(z_{ee} - z_{gg})/2$  and  $|z_{eg}|$  to represent the relative strength of the longitudinal and transverse spin-photon interactions, respectively. The unit of the absolute strength of the interactions can be regarded as  $eE_0/h \approx 0.1$  MHz/nm for  $E_0 = 0.4$  V/m.

### III. RESULTS IN AN INSB NANOWIRE QUANTUM DOT

In this section, we focus on the electron spin in an InSb nanowire quantum dot and its interaction with photons. Strong spin-orbit coupling is expected to exist in an InSb nanowire quantum dot, and a recent experiment has indeed reported a spin-orbit length of  $z_{\text{so}} = \hbar^2 / (m\alpha) \approx 230$  nm [48]. The spin manipulation frequency as large as 100 MHz by an external electric field has also been demonstrated [49]. For an InSb nanowire quantum dot, the effective electron mass in Eq. (1) reads  $m = 0.0136m_e$  [53], where  $m_e$  is the free electron mass, and the parameters  $\alpha$  and  $\delta$  in Eq. (1) can be simply interpreted as the Rashba spin-orbit coupling [54] and half of the Zeeman energy in a magnetic field, respectively. We have

$$\begin{aligned} \alpha &= \alpha(E), \\ \delta &= g_e \mu_B B / 2, \end{aligned} \quad (4)$$

where the Rashba spin-orbit coupling may be tunable by an external static electric field  $E$ , and  $g_e = -50.6$

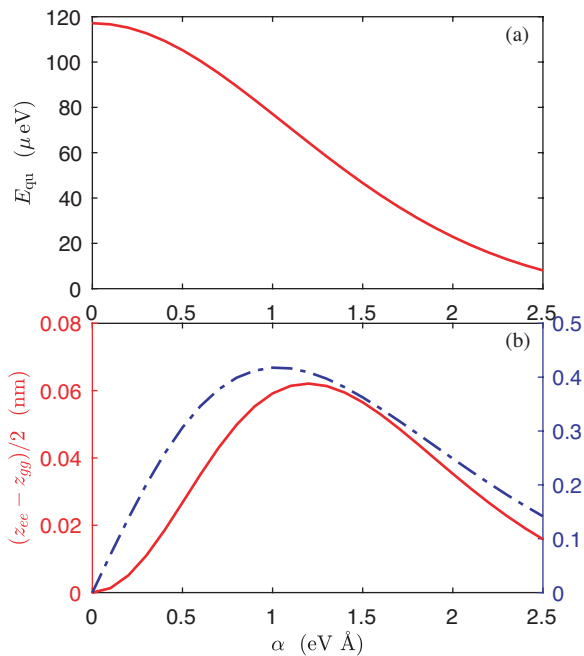


FIG. 2. (a) The spin splitting as a function of the spin-orbit coupling  $\alpha$ . (b) Both the longitudinal and the transverse spin-photon interactions as a function of the spin-orbit coupling  $\alpha$ . The magnetic field in the InSb quantum dot is chosen as  $B = 0.04$  T.

is the electron g-factor in InSb [55]. Note that  $\alpha$  may also contain a Dresselhaus spin-orbit coupling [56] contribution, this does not influence the form of Hamiltonian (1), because the Zeeman field can always be tuned to be perpendicular to the spin-orbit field for quasi-1D case.

We show in Fig. 2 the spin splitting  $E_{\text{qu}}$ , the longitudinal spin-photon interaction  $(z_{ee} - z_{gg})/2$ , and the transverse spin-photon interaction  $|z_{eg}|$  as a function of the spin-orbit coupling  $\alpha$ . Here, we have implicitly assumed  $\alpha$  is tunable by an external static electric field, and the magnetic field in Eq. (4) is fixed at  $B = 0.04$  T. With the increase of the spin-orbit coupling, the spin splitting  $E_{\text{qu}}$  decreases [see Fig. 2(a)], and both the longitudinal interaction  $(z_{ee} - z_{gg})/2$  and the transverse interaction  $|z_{eg}|$  first increase to a maximum and then decrease [see Fig. 2(b)]. Now, we can compare these results with that obtained in a symmetrical quantum dot. First, the spin-orbit coupling dependences of both  $E_{\text{qu}} \propto \exp(-z_{\text{size}}^2/z_{\text{so}}^2)$  and  $|z_{eg}| \propto z_{\text{size}}/z_{\text{so}} \exp(-z_{\text{size}}^2/z_{\text{so}}^2)$  are similar to that in a symmetrical quantum dot [8, 26, 57]. Here,  $z_{\text{size}}$  and  $z_{\text{so}} = \hbar^2/(m\alpha)$  are the quantum dot size (or characteristic length) and the spin-orbit length, respectively. Second, the longitudinal interaction  $(z_{ee} - z_{gg})/2$  can be observed only in an asymmetrical quantum dot.

In previous analytical studies in a symmetrical quantum dot, the Zeeman term  $\delta$  [see Eq. (4)] is treated as a perturbation, such that all the physical quantities obtained have a linear magnetic field dependence [8, 26, 57].

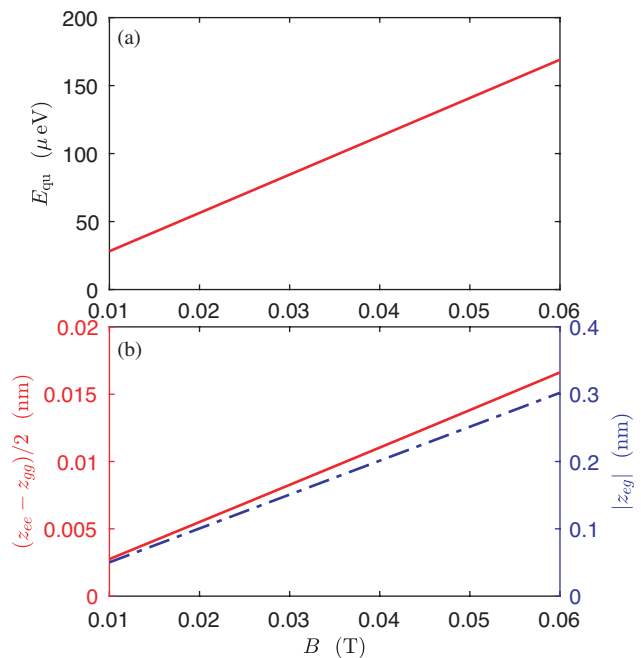


FIG. 3. (a) The spin splitting as a function of the magnetic field. (b) Both the longitudinal and the transverse spin-photon interactions as a function of the magnetic field. The spin-orbit coupling in the InSb quantum dot is chosen as  $\alpha = 0.3$   $\text{eV \AA}$  ( $z_{\text{so}} = 187$  nm).

Here, as expected, the spin splitting  $E_{\text{qu}}$ , the longitudinal spin-photon interaction  $(z_{ee} - z_{gg})/2$ , and the transverse spin-photon interaction  $|z_{eg}|$  all have a linear magnetic field dependence when the magnetic field is not very large (see Fig. 3). Here the spin-orbit coupling is set to a realistic value  $\alpha = 0.3$   $\text{eV \AA}$ , that corresponds to a spin-orbit length  $z_{\text{so}} = \hbar^2/(m\alpha) = 187$  nm, comparable with the experimentally observed value 230 nm [48]. Note that for this realistic spin-orbit coupling, the longitudinal interaction is almost one-order smaller than the transverse interaction [see Fig. 3(b)].

As we have emphasized that the longitudinal spin-photon interaction exists only in an asymmetrical quantum dot, now this assertion is unambiguously demonstrated in Fig. 4, where we show the spin splitting  $E_{\text{qu}}$ , the longitudinal spin-photon interaction  $(z_{ee} - z_{gg})/2$ , and the transverse spin-photon interaction  $|z_{eg}|$  as a function of the potential height  $V_2$ . When  $V_2 = 5$  meV, the confining potential is symmetrical, and the longitudinal interaction is zero [see Fig. 4(b)]. Here the spin-orbit coupling and magnetic field are chosen as  $\alpha = 0.3$   $\text{eV \AA}$  and  $B = 0.04$  T, respectively. In order to completely understand the results shown in Fig. 4, we should know that with the increase of the potential height  $V_2$ , not only does the degree of the asymmetry of the confining potential increase, but also the quantum dot size  $z_{\text{size}}$  decreases slightly. For  $\alpha = 0.3$   $\text{eV \AA}$ , the spin-orbit length  $z_{\text{so}} = \hbar^2/(m\alpha) = 187$  nm is much longer than the quantum dot size  $z_{\text{size}} \sim 40$  nm.

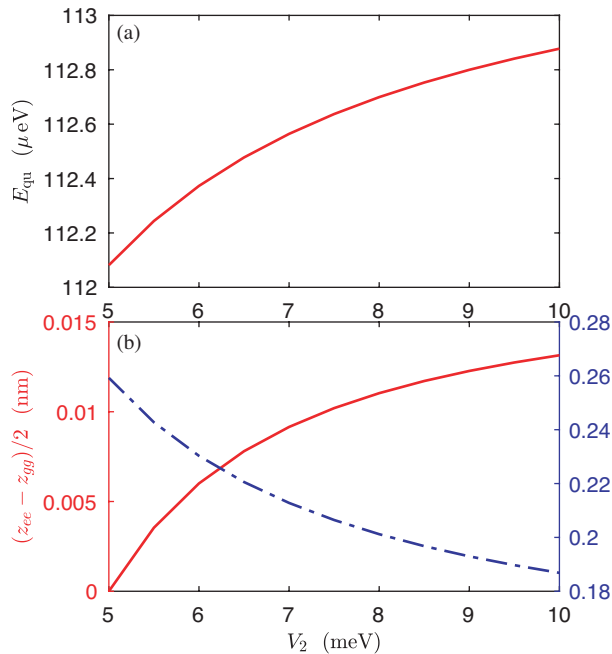


FIG. 4. (a) The spin splitting as a function of the potential height  $V_2$ . (b) Both the longitudinal and the transverse spin-photon interactions as a function of the potential height  $V_2$ . Here the other potential height is fixed at  $V_1 = 5$   $\text{meV}$ , and the spin-orbit coupling and magnetic field in the InSb quantum dot are chosen as  $\alpha = 0.3$   $\text{eV \AA}$  ( $z_{\text{so}} = 187$   $\text{nm}$ ) and  $B = 0.04$   $\text{T}$ , respectively.

When  $V_2$  increases, the quantum dot size decreases, such that  $E_{\text{qu}} \propto \exp(-z_{\text{size}}^2/z_{\text{so}}^2)$  increases [see Fig. 4(a)] and  $|z_{eg}| \propto z_{\text{size}}/z_{\text{so}} \exp(-z_{\text{size}}^2/z_{\text{so}}^2) \approx z_{\text{size}}/z_{\text{so}}$  decreases [see Fig. 4(b)] [8, 26]. While the longitudinal spin-photon interaction  $(z_{ee} - z_{gg})/2$ , resulting from the asymmetry of the confining potential, increases when  $V_2$  increases [see Fig. 4(b)]. Note that here the longitudinal interaction is still at least one-order smaller than the transverse interaction.

#### IV. RESULTS IN A GE NANOWIRE QUANTUM DOT

In this section, we focus on the hole pseudo spin in a Ge nanowire quantum dot and its interaction with photons. The hole in a cylindrical Ge nanowire has a peculiar low-energy subband structure, i.e., two shifted parabolic dispersions with an anticrossing at  $k_z = 0$  [58–61]. This result indicates that there is a natural strong pseudo spin-orbit coupling for hole due to the subband quantization [58, 60], although the real spin degeneracy still exists in the subband dispersions. If we split out the real spin degree of freedom by using a strong magnetic field [59], the induced lowest hole subband dispersion can be accurately described by the first three terms in Eq. (1) [60]. The spin-orbit coupling obtained in this

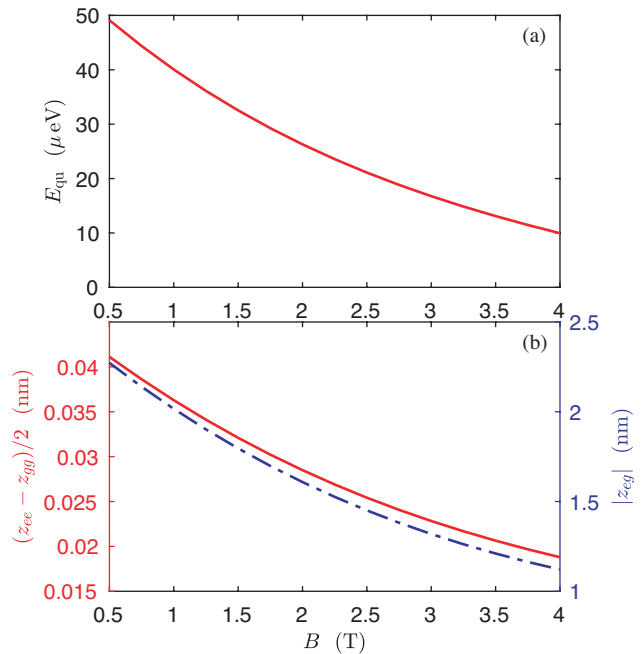


FIG. 5. (a) The spin splitting as a function of the magnetic field. (b) Both the longitudinal and the transverse spin-photon interactions as a function of the magnetic field.

way has the same form as that obtained by using a strong electric field to induce the structure inversion asymmetry in the nanowire [58, 62–64]. The main difference of these two spin-orbit couplings is that, one is in terms of the pseudo spin and depends on the external magnetic field [60], while the other is in terms of the real spin and depends on the external electric field [58, 64–68].

The interaction Hamiltonian between a Ge nanowire quantum dot and the cavity can still be written as Eq. (1). Now, the effective hole mass in Ge reads  $m \approx 0.074m_e$  [60], and both the parameters  $\alpha$  and  $\delta$  have non-trivial magnetic field dependence [60]

$$\begin{aligned} \alpha(B) &= C \frac{\hbar^2}{m_e R} - Z_3 \mu_B B R, \\ \delta(B) &= \frac{\Delta}{2} \frac{\hbar^2}{m_e R^2} - Z_1 \mu_B B + Z_4 \frac{e^2 B^2 R^2}{2m_e}, \end{aligned} \quad (5)$$

where  $C \approx 7.12$ ,  $\Delta \approx 0.77$ ,  $R$  is the radius of the nanowire,  $Z_1 = 0.75$ ,  $Z_3 = -3.62$ , and  $Z_4 = 0.65$  [58, 60]. Note that we have assumed the magnetic field is longitudinal, and the nanowire radius is set to  $R = 10$   $\text{nm}$  in the following calculations. The spin-orbit length  $z_{\text{so}} = \hbar^2/(m\alpha)$  in this case is about 16  $\sim$  19  $\text{nm}$  depending on the magnetic field strength [60], and it is less than the quantum dot width  $a = 40$   $\text{nm}$ .

We show in Fig. 5 the spin splitting  $E_{\text{qu}}$ , the longitudinal spin-photon interaction  $(z_{ee} - z_{gg})/2$ , and the transverse spin-photon interaction  $|z_{eg}|$  as a function of the longitudinal magnetic field  $B$ . With the increase of the magnetic field  $B$ , the spin-orbit coupling  $\alpha(B)$  increases while the Zeeman energy  $\delta(B)$  decreases [see Eq. (5)],

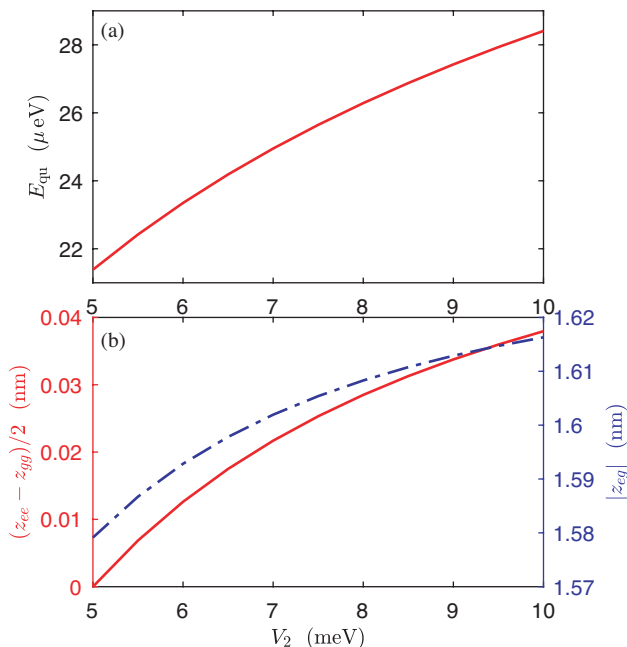


FIG. 6. (a) The spin splitting as a function of the potential height  $V_2$ . (b) Both the longitudinal and the transverse spin-photon interactions as a function of the potential height  $V_2$ . Here the other potential height is fixed at  $V_1 = 5$  meV and the magnetic field in the Ge quantum dot is chosen as  $B = 2$  T.

such that the spin splitting  $E_{\text{qu}}$  decreases reasonably [see Fig. 5(a)]. The results shown in Fig. 5(b) can be understood conveniently if we refer to the results shown in Fig. 2(b), that after the maximums of both  $(z_{ee} - z_{gg})/2$  and  $|z_{eg}|$ , these two quantities will decrease with the increase of  $\alpha$ . Here the spin-orbit length  $16 \sim 19$  nm in the Ge quantum dot is indeed smaller than the dot width  $a = 40$  nm, such that the situation here is indeed similar to that of the ultrastrong spin-orbit coupling region of the InSb quantum dot, e.g.,  $\alpha > 1.2$  eV  $\text{\AA}$  in Fig. 2(b). Therefore, with the increase of  $B$ , the spin-orbit coupling  $\alpha$  increases, it is reasonable to see both the longitudinal interaction  $(z_{ee} - z_{gg})/2$  and the transverse interaction  $z_{eg}$  decrease [see Fig. 5(b)]. We also note that the longitudinal interaction is at least one-order smaller than the transverse interaction. The order of the transverse interaction is 1 nm in terms of length  $|z_{eg}|$ , or 0.1 MHz in terms of frequency  $eE_0|z_{eg}|/h$ .

In Fig. 6, we show the potential height  $V_2$  dependence of the spin splitting  $E_{\text{qu}}$ , the longitudinal spin-photon interaction  $(z_{ee} - z_{gg})/2$ , and the transverse spin-photon interaction  $z_{eg}$ . We should keep in mind that when we vary the potential height  $V_2$ , both the quantum dot size and the degree of asymmetry of the potential are varied. With the increase of  $V_2$ , the quantum dot  $z_{\text{size}}$  decreases slightly, such that the level splitting  $E_{\text{qu}} \propto \exp(-z_{\text{size}}^2/z_{\text{so}}^2)$  increases [see Fig. 6(a)] [8, 26, 57]. Because the quantum dot is in the ultrastrong spin-orbit coupling region, that is similar to the case  $\alpha > 1.2$

eV  $\text{\AA}$  in Fig. 2(b), it is not difficult to understand  $|z_{eg}| \propto z_{\text{size}}/z_{\text{so}} \exp(-z_{\text{size}}^2/z_{\text{so}}^2)$  increases with the increase of  $V_2$  [see Fig. 6(b)] [8, 26]. While for the longitudinal spin-photon interaction  $(z_{ee} - z_{gg})/2$ , resulting from the asymmetry of the confining potential, increases with the increase of  $V_2$  [see Fig. 6(b)]. Also, when  $V_2 = 5$  meV, the confining potential is symmetrical, there is no longitudinal spin-photon interaction. Note that here the longitudinal interaction is still at least one-order smaller than the transverse interaction.

## V. CHARGE NOISE INDUCED SPIN DEPHASING

In Eq. (3),  $(z_{ee} + z_{gg})/2$  can be interpreted as the equilibrium point of the electron or hole in an asymmetrical confining potential. If we take this equilibrium point into account in the electric-dipole interaction  $e[z - (z_{ee} + z_{gg})/2]E_c$ , the  $(z_{ee} + z_{gg})/2$  term in Eq. (3) will disappear. We now generalize Eq. (3) to the case of the spin-charge-noise interaction, where  $\mathbf{E}_c$  is replaced by a fluctuating charge field  $\sum_k E_k(b_k + b_k^\dagger)$ . The longitudinal spin-charge interaction induces spin dephasing ( $T_2$ ), while the transverse spin-charge interaction induces spin relaxation ( $T_1$ ). For quantum dot spin qubit, the dephasing time is usually much less than the relaxation time  $T_2 \ll T_1$  [69].

Here we focus only on the dephasing time of the spin qubit, such that we have the following effective interaction Hamiltonian

$$H_{\text{ef}} = \frac{E_{\text{qu}}}{2} \tilde{\sigma}^z + e \frac{z_{ee} - z_{gg}}{2} \tilde{\sigma}^z \sum_k E_k (b_k + b_k^\dagger) + \sum_k \hbar \omega_k b_k^\dagger b_k. \quad (6)$$

The off-diagonal element of the reduced density matrix of the spin qubit governed by Hamiltonian (6) can be solved as  $\rho_{\uparrow\downarrow}(t) = \rho_{\uparrow\downarrow}(0) \exp[-\Gamma(t)]$ , where [21, 22]

$$\Gamma(t) = \sum_k \frac{2(z_{ee} - z_{gg})^2 e^2 E_k^2 \sin^2 \frac{\omega_k t}{2}}{\hbar^2 \omega_k^2} [2n(\omega_k) + 1], \quad (7)$$

with  $n(\omega_k) = 1/[\exp(\hbar\omega_k/k_B T) - 1]$  being the thermal average boson number.

In order to obtain the dephasing time of the spin qubit, one has to assume a strength of the spectrum function of the charge noise [21, 22], a quantity related to the series of  $E_k$  values in Eq. (6). Here, we will not do this calculation by artificially choosing a strength of the spectrum function, we just compare the dephasing time of the spin qubit with that of the charge qubit in a double quantum dot. When the noise frequency spectrum has both lower bound  $\omega_{\text{min}}$  and upper bound  $\omega_{\text{max}}$  such as the  $1/f$  charge noise [70], i.e.,  $\omega_k \in [\omega_{\text{min}}, \omega_{\text{max}}]$ , for time scales  $t < 1/\omega_{\text{max}}$ , we can safely make the following approximation  $\sin^2 \omega_k t/2 \approx \omega_k^2 t^2/4$  in Eq. (7), such that we have

$$\Gamma(t) \propto (z_{ee} - z_{gg})^2 t^2. \quad (8)$$

For a charge qubit in double quantum dot,  $(z_{ee} - z_{gg})_{\text{charge}}$  has an order of magnitude of the interdot distance, the typical value is about several tens of nm, while for the spin qubit considered here,  $(z_{ee} - z_{gg})_{\text{spin}}$  has an order of magnitude of  $10^{-2}$  nm. Thus, it is reasonable to have the following relation  $(z_{ee} - z_{gg})_{\text{spin}} \approx 10^{-3}(z_{ee} - z_{gg})_{\text{charge}}$ . A rough analysis of Eq. (8) gives rise to  $T_2^{\text{spin}} \approx 10^3 T_2^{\text{charge}}$ . Typical charge qubit dephasing time has an order of ns [71, 72], such that the spin qubit dephasing time is likely to have an order of  $\mu\text{s}$ .

## VI. DISCUSSION AND SUMMARY

The longitudinal interaction mechanism between the spin qubit and photons in our paper is somewhat similar to that between the charge qubit and photons in a double quantum dot, where the two unequal interdot charge energies play an essential role [45, 71], e.g., the double dot confining potential is asymmetrical. Spin-photon interaction can also be mediated by a synthetic spin-orbit coupling [27, 35, 36, 73], e.g., created by a gradient magnetic field. The exchange gate [35] and iSWAP gate [36] between spin qubits can further be mediated via virtual microwave photons, and optimal operating regimes for an iSWAP gate were revealed [36]. Although our paper focuses on the static longitudinal spin-photon interaction, the dynamic longitudinal spin-photon interaction, i.e., induced by an external driving field, is also a very active research field [44, 45]. Let us also discuss on the magnitude of the transverse spin-photon interaction (in terms of length). The charge-photon interaction has an order

of the quantum dot size, i.e., 40 nm in our paper. While the spin-photon interaction, mediated by the spin-orbit coupling, must be much smaller than the charge-photon interaction. Our calculated spin-photon interaction has an order of magnitude of 1 nm, hence is very reasonable.

In summary, via exactly solving the spin basis states, we obtain not only a transverse spin-photon interaction but also a longitudinal spin-photon interaction in an asymmetrical nanowire quantum dot. For both electron spin in an InSb nanowire quantum dot and hole pseudo spin in a Ge nanowire quantum dot, we calculate the dependences of the spin splitting, and both the transverse and the longitudinal spin-photon interactions on a series of external tunable parameters. For realistic spin-orbit coupling and realistic quantum dot parameters, the longitudinal interaction is at least one-order smaller than the transverse interaction. The longitudinal spin-photon interaction results from the confined effects of spin-orbit coupling and the asymmetrical confining potential. There is no longitudinal spin-photon interaction in a symmetrical quantum dot. The longitudinal spin-electric interaction demonstrated here may provide a mechanism for the charge noise induced spin dephasing in semiconductor quantum dot [21, 22].

## ACKNOWLEDGEMENTS

This work was supported by the National Natural Science Foundation of China Grant No. 11404020, the Project from the Department of Education of Hebei Province Grant No. QN2019057, and the Starting up Foundation from Yanshan University Grant No. BL18043.

- 
- [1] D. Loss and D. P. DiVincenzo, Quantum computation with quantum dots, *Phys. Rev. A* **57**, 120 (1998).
  - [2] L. M. K. Vandersypen and M. A. Eriksson, Quantum computing with semiconductor spins, *Physics Today* **72**, 38 (2019).
  - [3] G. Scappucci, C. Kloeffel, F. A. Zwanenburg, D. Loss, M. Myronov, J.-J. Zhang, S. De Franceschi, G. Katsaros, and M. Veldhorst, The germanium quantum information route, *Nature Reviews Materials* **6**, 926 (2021).
  - [4] G. Burkard, T. D. Ladd, A. Pan, J. M. Nichol, and J. R. Petta, Semiconductor spin qubits, *Rev. Mod. Phys.* **95**, 025003 (2023).
  - [5] E. I. Rashba and A. L. Efros, Orbital mechanisms of electron-spin manipulation by an electric field, *Phys. Rev. Lett.* **91**, 126405 (2003).
  - [6] V. N. Golovach, M. Borhani, and D. Loss, Electric-dipole-induced spin resonance in quantum dots, *Phys. Rev. B* **74**, 165319 (2006).
  - [7] D. V. Bulaev and D. Loss, Electric dipole spin resonance for heavy holes in quantum dots, *Phys. Rev. Lett.* **98**, 097202 (2007).
  - [8] R. Li, J. Q. You, C. P. Sun, and F. Nori, Controlling a nanowire spin-orbit qubit via electric-dipole spin resonance, *Phys. Rev. Lett.* **111**, 086805 (2013).
  - [9] J. Romhányi, G. Burkard, and A. Pályi, Subharmonic transitions and bloch-siegert shift in electrically driven spin resonance, *Phys. Rev. B* **92**, 054422 (2015).
  - [10] Z. Wang, E. Marcellina, A. R. Hamilton, J. H. Cullen, S. Rogge, J. Salfi, and D. Culcer, Optimal operation points for ultrafast, highly coherent Ge hole spin-orbit qubits, *npj Quantum Information* **7**, 54 (2021).
  - [11] D. Khomitsky, E. Lavrakhina, and E. Sherman, Spin rotation by resonant electric field in few-level quantum dots: Floquet dynamics and tunneling, *Phys. Rev. Applied* **14**, 014090 (2020).
  - [12] G. Burkard, D. Loss, and D. P. DiVincenzo, Coupled quantum dots as quantum gates, *Phys. Rev. B* **59**, 2070 (1999).
  - [13] X. Hu and S. Das Sarma, Hilbert-space structure of a solid-state quantum computer: Two-electron states of a double-quantum-dot artificial molecule, *Phys. Rev. A* **61**, 062301 (2000).
  - [14] E. Kawakami, T. Jullien, P. Scarlino, D. R. Ward, D. E. Savage, M. G. Lagally, V. V. Dobrovitski, M. Friesen, S. N. Coppersmith, M. A. Eriksson, and L. M. K. Vandersypen, Gate fidelity and coherence of an electron spin in a Si/SiGe quantum dot with micromagnet, *Proceedings of the National Academy of Sciences* **113**, 11738 (2016).

- [15] J. Yoneda, K. Takeda, T. Otsuka, T. Nakajima, M. R. Delbecq, G. Allison, T. Honda, T. Koderu, S. Oda, Y. Hoshi, *et al.*, A quantum-dot spin qubit with coherence limited by charge noise and fidelity higher than 99.9%, *Nature nanotechnology* **13**, 102 (2018).
- [16] W. M. Witzel and S. Das Sarma, Quantum theory for electron spin decoherence induced by nuclear spin dynamics in semiconductor quantum computer architectures: Spectral diffusion of localized electron spins in the nuclear solid-state environment, *Phys. Rev. B* **74**, 035322 (2006).
- [17] W. Yao, R.-B. Liu, and L. J. Sham, Theory of electron spin decoherence by interacting nuclear spins in a quantum dot, *Phys. Rev. B* **74**, 195301 (2006).
- [18] A. V. Khaetskii and Y. V. Nazarov, Spin relaxation in semiconductor quantum dots, *Phys. Rev. B* **61**, 12639 (2000).
- [19] A. V. Khaetskii and Y. V. Nazarov, Spin-flip transitions between zeeman sublevels in semiconductor quantum dots, *Phys. Rev. B* **64**, 125316 (2001).
- [20] A. Bermeister, D. Keith, and D. Culcer, Charge noise, spin-orbit coupling, and dephasing of single-spin qubits, *Applied Physics Letters* **105**, 192102 (2014).
- [21] R. Li, A spin dephasing mechanism mediated by the interplay between the spin-orbit coupling and the asymmetrical confining potential in a semiconductor quantum dot, *Journal of Physics: Condensed Matter* **30**, 395304 (2018).
- [22] R. Li, Charge noise induced spin dephasing in a nanowire double quantum dot with spin-orbit coupling, *Journal of Physics: Condensed Matter* **32**, 025305 (2020).
- [23] M. O. Scully and M. S. Zubairy, *Quantum optics* (Cambridge University Press, Cambridge, England, 1997).
- [24] E. Jaynes and F. Cummings, Comparison of quantum and semiclassical radiation theories with application to the beam maser, *Proceedings of the IEEE* **51**, 89 (1963).
- [25] I. I. Rabi, On the process of space quantization, *Phys. Rev.* **49**, 324 (1936).
- [26] M. Trif, V. N. Golovach, and D. Loss, Spin dynamics in InAs nanowire quantum dots coupled to a transmission line, *Phys. Rev. B* **77**, 045434 (2008).
- [27] X. Hu, Y.-x. Liu, and F. Nori, Strong coupling of a spin qubit to a superconducting stripline cavity, *Phys. Rev. B* **86**, 035314 (2012).
- [28] C. Kloeffel, M. Trif, P. Stano, and D. Loss, Circuit QED with hole-spin qubits in Ge/Si nanowire quantum dots, *Phys. Rev. B* **88**, 241405 (2013).
- [29] P. M. Mutter and G. Burkard, Cavity control over heavy-hole spin qubits in inversion-symmetric crystals, *Phys. Rev. B* **102**, 205412 (2020).
- [30] P.-Q. Jin, M. Marthaler, A. Shnirman, and G. Schön, Strong coupling of spin qubits to a transmission line resonator, *Phys. Rev. Lett.* **108**, 190506 (2012).
- [31] Y. Li, S.-X. Li, F. Gao, H.-O. Li, G. Xu, K. Wang, D. Liu, G. Cao, M. Xiao, T. Wang, J.-J. Zhang, G.-C. Guo, and G.-P. Guo, Coupling a germanium hut wire hole quantum dot to a superconducting microwave resonator, *Nano Letters* **18**, 2091 (2018).
- [32] G. Burkard, M. J. Gullans, X. Mi, and J. R. Petta, Superconductor-semiconductor hybrid-circuit quantum electrodynamics, *Nature Reviews Physics* **2**, 129 (2020).
- [33] V. P. Michal, J. C. Abadillo-Uriel, S. Zihlmann, R. Maurand, Y.-M. Niquet, and M. Filippone, Tunable hole spin-photon interaction based on  $g$ -matrix modulation, *Phys. Rev. B* **107**, L041303 (2023).
- [34] S. Bosco, P. Scarlino, J. Klinovaja, and D. Loss, Fully tunable longitudinal spin-photon interactions in Si and Ge quantum dots, *Phys. Rev. Lett.* **129**, 066801 (2022).
- [35] P. Harvey-Collard, J. Dijkema, G. Zheng, A. Sammak, G. Scappucci, and L. M. K. Vandersypen, Coherent spin-spin coupling mediated by virtual microwave photons, *Phys. Rev. X* **12**, 021026 (2022).
- [36] S. M. Young, N. T. Jacobson, and J. R. Petta, Optimal control of a cavity-mediated iSWAP gate between silicon spin qubits, *Phys. Rev. Appl.* **18**, 064082 (2022).
- [37] A. Imamoglu, D. D. Awschalom, G. Burkard, D. P. DiVincenzo, D. Loss, M. Sherwin, and A. Small, Quantum information processing using quantum dot spins and cavity qed, *Phys. Rev. Lett.* **83**, 4204 (1999).
- [38] S.-B. Zheng and G.-C. Guo, Efficient Scheme for Two-Atom Entanglement and Quantum Information Processing in Cavity QED, *Phys. Rev. Lett.* **85**, 2392 (2000).
- [39] A. Blais, R.-S. Huang, A. Wallraff, S. M. Girvin, and R. J. Schoelkopf, Cavity quantum electrodynamics for superconducting electrical circuits: An architecture for quantum computation, *Phys. Rev. A* **69**, 062320 (2004).
- [40] A. Blais, A. L. Grimsmo, S. M. Girvin, and A. Wallraff, Circuit quantum electrodynamics, *Rev. Mod. Phys.* **93**, 025005 (2021).
- [41] K. D. Petersson, L. W. McFaul, M. D. Schroer, M. Jung, J. M. Taylor, A. A. Houck, and J. R. Petta, Circuit quantum electrodynamics with a spin qubit, *Nature* **490**, 380 (2012).
- [42] N. Samkharadze, G. Zheng, N. Kalhor, D. Brousse, A. Sammak, U. C. Mendes, A. Blais, G. Scappucci, and L. M. K. Vandersypen, Strong spin-photon coupling in silicon, *Science* **359**, 1123 (2018).
- [43] C. X. Yu, S. Zihlmann, J. Abadillo-Uriel, V. P. Michal, N. Rambal, H. Niebojewski, T. Bedecarrats, M. Vinet, É. Dumur, M. Filippone, B. Bertrand, S. De Franceschi, Y.-M. Niquet, and R. Maurand, Strong coupling between a photon and a hole spin in silicon, *Nature Nanotechnology* **18**, 741 (2023).
- [44] C. G. L. Böttcher, S. P. Harvey, S. Fallahi, G. C. Gardner, M. J. Manfra, U. Vool, S. D. Bartlett, and A. Yacoby, Parametric longitudinal coupling between a high-impedance superconducting resonator and a semiconductor quantum dot singlet-triplet spin qubit, *Nature Communications* **13**, 4773 (2022).
- [45] J. Corrigan, B. Harpt, N. Holman, R. Ruskov, P. Marciniak, D. Rosenberg, D. Yost, R. Das, W. D. Oliver, R. McDermott, C. Tahan, M. Friesen, and M. Eriksson, Longitudinal coupling between a  $\text{Si/Si}_{1-x}\text{Ge}_x$  double quantum dot and an off-chip TiN resonator, *Phys. Rev. Appl.* **20**, 064005 (2023).
- [46] R. Li, Z. H. Liu, Y. Wu, and C. S. Liu, The impacts of the quantum-dot confining potential on the spin-orbit effect, *Sci Rep* **8**, 7400 (2018).
- [47] Y. Ban, X. Chen, J. G. Muga, and E. Y. Sherman, Quantum state engineering of spin-orbit-coupled ultracold atoms in a morse potential, *Phys. Rev. A* **91**, 023604 (2015).
- [48] S. Nadj-Perge, V. S. Pribiag, J. W. G. van den Berg, K. Zuo, S. R. Plissard, E. P. A. M. Bakkers, S. M. Frolov, and L. P. Kouwenhoven, Spectroscopy of spin-orbit quantum bits in indium antimonide nanowires, *Phys. Rev. Lett.* **108**, 166801 (2012).

- [49] J. W. G. van den Berg, S. Nadj-Perge, V. S. Pribiag, S. R. Plissard, E. P. A. M. Bakkers, S. M. Frolov, and L. P. Kouwenhoven, Fast spin-orbit qubit in an indium antimonide nanowire, *Phys. Rev. Lett.* **110**, 066806 (2013).
- [50] F. N. M. Froning, L. C. Camenzind, O. A. H. van der Molen, A. Li, E. P. A. M. Bakkers, D. M. Zumbühl, and F. R. Braakman, Ultrafast hole spin qubit with gate-tunable spin-orbit switch functionality, *Nature Nanotechnology* **16**, 308 (2021).
- [51] K. Wang, G. Xu, F. Gao, H. Liu, R.-L. Ma, X. Zhang, Z. Wang, G. Cao, T. Wang, J.-J. Zhang, D. Culcer, X. Hu, H.-W. Jiang, H.-O. Li, G.-C. Guo, and G.-P. Guo, Ultrafast coherent control of a hole spin qubit in a germanium quantum dot, *Nature Communications* **13**, 206 (2022).
- [52] F. M. Gambetta, N. T. Ziani, S. Barbarino, F. Cavaliere, and M. Sassetti, Anomalous friedel oscillations in a quasi-helical quantum dot, *Phys. Rev. B* **91**, 235421 (2015).
- [53] O. Madelung, *Semiconductors: data handbook* (Springer Science & Business Media, 2004).
- [54] Y. A. Bychkov and E. I. Rashba, Oscillatory effects and the magnetic susceptibility of carriers in inversion layers, *Journal of Physics C: Solid State Physics* **17**, 6039 (1984).
- [55] E. Tsitsishvili, G. S. Lozano, and A. O. Gogolin, Rashba coupling in quantum dots: An exact solution, *Phys. Rev. B* **70**, 115316 (2004).
- [56] G. Dresselhaus, Spin-orbit coupling effects in zinc blende structures, *Phys. Rev.* **100**, 580 (1955).
- [57] M. P. Nowak and B. Szafran, Spin-polarization anisotropy in a narrow spin-orbit-coupled nanowire quantum dot, *Phys. Rev. B* **87**, 205436 (2013).
- [58] C. Kloeffel, M. Trif, and D. Loss, Strong spin-orbit interaction and helical hole states in Ge/Si nanowires, *Phys. Rev. B* **84**, 195314 (2011).
- [59] R. Li, Searching strong ‘spin’-orbit coupled one-dimensional hole gas in strong magnetic fields, *Journal of Physics: Condensed Matter* **34**, 075301 (2022).
- [60] R. Li and X.-Y. Qi, Two-band description of the strong ‘spin’-orbit coupled one-dimensional hole gas in a cylindrical Ge nanowire, *Journal of Physics: Condensed Matter*, **35**, 135302 (2023).
- [61] R. Li and Z.-Q. Li, Low-energy hole subband dispersions in a cylindrical Ge nanowire: the effects of the nanowire growth direction, *Journal of Physics: Condensed Matter*, **35**, 345301 (2023).
- [62] C. Kloeffel, M. J. Rančić, and D. Loss, Direct rashba spin-orbit interaction in Si and Ge nanowires with different growth directions, *Phys. Rev. B* **97**, 235422 (2018).
- [63] J.-W. Luo, L. Zhang, and A. Zunger, Absence of intrinsic spin splitting in one-dimensional quantum wires of tetrahedral semiconductors, *Phys. Rev. B* **84**, 121303 (2011).
- [64] J.-W. Luo, S.-S. Li, and A. Zunger, Rapid transition of the hole rashba effect from strong field dependence to saturation in semiconductor nanowires, *Phys. Rev. Lett.* **119**, 126401 (2017).
- [65] F. Maier, J. Klinovaja, and D. Loss, Majorana fermions in Ge/Si hole nanowires, *Phys. Rev. B* **90**, 195421 (2014).
- [66] M. Milivojević, Electrical control of the hole spin qubit in Si and Ge nanowire quantum dots, *Phys. Rev. B* **104**, 235304 (2021).
- [67] C. Adelsberger, M. Benito, S. Bosco, J. Klinovaja, and D. Loss, Hole-spin qubits in Ge nanowire quantum dots: Interplay of orbital magnetic field, strain, and growth direction, *Phys. Rev. B* **105**, 075308 (2022).
- [68] C. Adelsberger, S. Bosco, J. Klinovaja, and D. Loss, Enhanced orbital magnetic field effects in Ge hole nanowires, *Phys. Rev. B* **106**, 235408 (2022).
- [69] I. Buluta, S. Ashhab, and F. Nori, Natural and artificial atoms for quantum computation, *Reports on Progress in Physics* **74**, 104401 (2011).
- [70] E. Paladino, Y. M. Galperin, G. Falci, and B. L. Altshuler,  $1/f$  noise: Implications for solid-state quantum information, *Rev. Mod. Phys.* **86**, 361 (2014).
- [71] T. Hayashi, T. Fujisawa, H. D. Cheong, Y. H. Jeong, and Y. Hirayama, Coherent manipulation of electronic states in a double quantum dot, *Phys. Rev. Lett.* **91**, 226804 (2003).
- [72] J. Gorman, D. G. Hasko, and D. A. Williams, Charge-qubit operation of an isolated double quantum dot, *Phys. Rev. Lett.* **95**, 090502 (2005).
- [73] R. Li, Spin manipulation and spin dephasing in quantum dot integrated with a slanting magnetic field, *Physica Scripta* **94**, 085808 (2019).